Journal of scientific research

Refereed scientific journal

Issued twice annually by:

Africa University for humanities
and applied sciences

Tripoli-libya

Issue No.(3), Second year 2017

Journal of Scientific Research Issued By:

Africa University for Human and Applied Sciences

Libya - 2016

Journal of Scientific Research Issued By:

Africa University for Human and Applied Sciences

General Advisor

Dr.Mabruk Muftah Abushina

Head of the Editorial Committee

Dr. Abdin A. Sharif

Members of the Editorial Committee

Dr. Abdelhamed Ali Magrus

.Salah Almbrouk Khalel

.Akram H. Mom Moamer

Abdarzag Almabrok Alkanony .

Journal of Scientific Research Issued By:

Africa University for human and Applied Sciences

Principles and Regulation

A brief about the Journal

It is an evaluated-based, quarterly journal issued **Africa University for human and Applied Sciences** – Libya - in Arabic and English. It is interested in publishing research papers and scientific studies, as well as, presenting books and periodicals summaries, Doctorate or Master Theses, conferences and workshops reporters inside and outside Libya.

Journal Objectives

Activating and enriching scientific research in all scientific fields related to the University majors Paying attention to the comprehensive development issues in the light of the local, regional and international changes offering a chance for researchers to publish their studies and to convey their ideas in order to expand the circle of knowledge among researchers, decision makers and practitioners inside and outside Libya creating a scientific dialogue among researchers and those who are interested in updated issues in all scientific fields related to the University majors

Publishing principles, regulations and criteria

Studies and research papers presented to publication in the journal should accordance with the following principles and regulations:

1. **Research and studies**:

These should be :

- ✓ original in terms of the research ideas and them; they should neither be published nor part of a Doctorate or a Master thesis
- ✓ written in a correct methodology and
- ✓ written in a clear and correct language; they should be coherent and cohesive

2. **Referencing:**

Sources should be cited and documented chronologically accordance with the following:

- ✓ **Reference to a book**

Elements to cite:
Full name of the author, title of the book, place of publication, publisher, year and page/s.

- ✓ **Reference to an article in a journal**

Elements to cite:
Full name of the author, name of the journal, volume number, date of publication, research or article pages:

- ✓ **Reference to indirect quotation (a contribution in a book):** cite the original source

3. **Footnotes:**

Footnotes are restricted to explaining or clarifying ambiguous points which cannot be included in text and in order to be highlighted. Each page should be numbered independently. Footnotes should appear at the bottom of the page.

4. References and bibliography:

Arabic references should be cited first. References should include only what have been actually cited in text by the researcher. They should be ordered alphabetically as follows:

First: Arabic references

- المهدي غنية مبادئ التسويق، (طرابلس: الجامعة المفتوحة (2002).
- عبد السلام ابوقحف مقدمة في إدارة الأعمال الدولية، (الإسكندرية: مطبعة الإشعاع الفنية (1998)
- محمد المكي "أهمية المراقبة الداخلية للمراجع الخارجي"، (طرابلس: مجلة دراسات في الإدارة والأعمال المصرفية)، العدد 6 (1984)، ص ص: 15-18.

Second: foreign references

- Drury, Colin (2000), Management and Cost Accounting, 5th edition, (London: Thomson Learning).
- Kaplan, Robert (2000), Balance without profit, Financial Management, (January), 23-26

Third: Material from the Web

For citing material from the Web, two additional pieces of information are usually needed:

- **The electronic address or URL of the site (e.g. http ://...)**
- **the date you accessed the site or database**

5. General and technical principles:

- ✓ Researchers should write their names, degrees, occupations, place of work in the first page of their

research. It is also important to mention the correspondent address, fax and phone number, and e-mail.

- ✓ Research papers and studies should be written in Arabic and English provided that a summary in Arabic, of not more than 150 words, is enclosed.
- ✓ the number of pages, including tables, references, and graphs should not exceed 20 pages
- ✓ Research papers and studies should be printed in Microsoft Word on one side paper of (A4) single-spaced. A (CD) of the work and a Curriculum Vita (CV) of the researcher should be enclosed.
- ✓ Works presented in Arabic should be in **(Simplified Arabic)**.Works presented in English should be in **(Times New Roman)**.
- ✓ Font size should be as follows:
    - Size 18 for the main headlines
    - Size 16 for the subtitles
    - Size 14 for the text
    - Size 12 for the abstract in *italic*
    - Size 10 for the footnotes
- ✓ Margins should be as follows:
    - Up and bottom 2.5 cm
    - Right 3 cm
    - Left 2.5 cm

The research papers and the studies presented to the journal are subject to the evaluation by specialized professors assigned confidentially by the editorial committee. The journal has the right to ask the researcher to make the necessary corrections required by the evaluators. The journal has the right to make minor correction, when necessary, without an advanced permission from the researcher. The editorial committee has the right to seek assistance of more than one referee if necessary and the researchers will be informed whether their work has been accepted or not according to the referees' reports.

Unaccepted works for publication will not be returned to the researchers.

The researcher vow never to publish the research or the study by any other means for a period of two years from the date of publishing.

All points of view published in the journal represent the writers and do not necessarily represent the view of the journal.

The journal assures to inform the researcher with receiving and forwarding his work to the editorial committee in two weeks time.

The journal assures to inform the researcher of the acceptance of his work in two weeks time from receiving the referrers' reply.

The journal informs the researcher in which issue the work will be published.

Publication rights will be transferred to the journal when the researcher is informed of the acceptance of his work.

Publishing of research or studies in the journal is ordered according to the technical considerations, and to the submission date, not to the importance of the work or status of the researcher.

The researcher obtains three copies of the issue when his research or study is published.

6. Correspondence addresses:

All studies, research and correspondences should be sent to the Head of the Editorial Committee of **University Journal of Scientific Research:**

Africa University for human and Applied Sciences

On the following address: P. pox 83060 Tripoli – Libya

E-mail: Info@africanuniversityedu.ly

Phone: +218217291428- **Fax**: +218217291428

The University web site: www. africuniversityedu.ly

Content Issue No. 3

Effect of austenitizing condition on carbon content and volume fraction of austenite of an alloyed ADI

Jihan Eldaour , jihansedo@gmail .com

Alzzatuna University, Engineering Faculty

الملخص

تم في هذا البحث دراسة عينات من الحديد المطاوع تحتوي على عناصر سبائكية (نحاس و نيكل بنسبة 1.6% لكلا منهما) خضعت لمعالجة حرارية تدعى (austempering) عند درجة حرارة ثابتة 360°م و لزمن ثابت 180 دقيقة, بعد معالجة حرارية تدعى (austenitizing) للوصول بالسبيكة لطور الأوستينيت لدرجتي حرارة مختلفتين (900, 1000°م) و لأزمان مختلفة أيضا. مبتدئا من 15 دقيقة, 60, 120, و منتهيا بـ 180 دقيقة. و دراستنا تهتم بتأثير ظروف المعالجة (الحرارة و الزمن) على المحتوى الكربوني C_γ و كذلك تأثيرها على كمية الأوستينيتX_γ , حاصل ضرب كمية الأوستينيت و محتواها الكربوني $X_\gamma C_\gamma$ و أخيرا على حجم الفيرايت الأبري. و باستخدام حيود الأشعة السينية لتقدير كلا من: كمية الأوستينيت X_γ , و نسبة الكربون بداخلهC_γ و كذلك حاصل ضربهما ($X_\gamma C_\gamma$) بأتباع خطوات طريقة كلا من Rundman و Klug و أخيرا حساب حجم حبيبات الفيرايت باستخدام Scherrer formula. لوحظ من خلال النتائج أن المحتوى الكربوني داخل الأوستينيت يزداد بزيادة زمن التسخين لطور الأوستينيت و أن كمية الأوستينيت المتبقي و الثابت عند درجة حرارة الغرفة يزداد بزيادة كلا من الزمن و درجة الحرارة. أما عن تأثير المعالجة الحرارية (austenitizing) على التركيب المجهري للعينات فقد تم دراسته و لوحظ أن هناك تغير ملحوظ في شكل و حجم الفيرايت الأبري و كذلك مظهر الأوستينيت المتبقي, حيث أن الأوستينيت يظهر على شكل رقائق فضية متداخلة بين الفيرايت الأبري و كذلك بمظهر كتلي أيضا. وأن أفضل زمن لعملية (austenitizing) و التي تتطابق مع أفضل تركيب مجهري مرغوب فيه عند 180 ثم 120 دقيقة.

Abstract

A ductile iron containing 1.6 wt% Cu and 1.6 wt% Ni as the main alloying elements was austempered at a fixed austempering temperature of 360°C for a fixed austempering time of 180 min after austenitizing at 900°C for different austenitizing periods of 15, 30, 60, 120, and 180 min. the austempering process was repeated after changing austenitizing temperature to 1000°C. The effect of austenitizing temperature and time was studied on structural parameters like the carbon content in austenite C_γ after austenitizing, the volume fraction of austenite after austentizing X_γ, their product $X_\gamma C_\gamma$, and the ferrite needle size d_α after austempering.

X-ray diffraction analysis was performed to estimate the percentage of carbon in austenite C_γ, the austenite content X_γ, following the procedure of Rundman and Klug, and so the particle size d_α, have been investigated by using the Scherrer formula.

The carbon content in austenite increases with increasing the austenitizing time, and so the amount of retained austenite increases with increasing both times and temperatures. The effect of austenitizing parameters were also studied on austempered microstrucure.

The qualitative variation in morphology, size of ferrite needles and retained austenite in austempered microstructure with austenitizing conditions were observed.

The austenitizing conditions not only affect the morphology of ferrite but the retained austenite. Austenite appears to exist in the form of films between ferrite needles, as well as in blocky morphology.

The austenitization time corresponding to most desirable austempered microstructure is 180 followed by 120 min.

1- Introduction

Austempered ductile cast iron (ADI) has a better combination of strength, ductility, toughness, fatigue and wear resistance. Thus, it is considered an important engineering material, that is useful in a great number of applications. Many applications of ADI have been reported earlier [1-4]. ADI is obtained by subjecting the ductile cast iron to austempering heat-treatment cycle. The austempering reactions in ADI occur in two stages [5]. In stageI, the matrix austenite with carbon content $C°_\gamma$ isothermally transforms into ausferrite, i.e., into a mixture of acicular ferrite with carbon enriched stabilized austenite with carbon content C_γ%. In stageII, the stabilized austenite decomposes into ferrite and carbide. Previous investigators [6-8] have studied the effects of austenitising temperature (T_γ), austempering temperature (T_A) and austempering time (t_A) on the structure and mechanical properties of this material but very little work has been carried out on the influence of

austenitising time (t_γ). Thus this work studies the austenitizing transformations and microstructural changes during austempering of alloyed ductile iron. Data from the literature have been analyzed to understand aspect of the retained austenite in austempered ductile irons. The current study deals with the effect of austenitization temperature and time on the average carbon content and volume fraction of austenite after austempering.

2- Experimental Procedure

2.1- Material and Heat treatment

The ductile cast iron (DI) used in the present work has the following chemical composition (wt. %): 3.3C, 2.6 Si, 0.35Mn, 0.008S, 0.01P. 0.05Mg, 1.6Cu, 1.6Ni, balance Fe. It was supplied in the form of round cylindrical (20mm) diameter and 5mm long specimens made of this DI were subjected to cycle heat treatment to produce austempered ductile cast iron: austenitizing at 900°C and 1000°C for different times at each temperature (15, 30, 60, 120, and 180 min), then austempering at 360°C for 180 min in a salt bath with subsequent cooling to ambient temperature to prevent any transformations of austenite into pearlite. The resulting microstructure contained a ferritic matrix with some spheroidized carbides and graphite spheres. The latter have nodularity in excess of 90% and an average diameter of 0.045 mm. The graphite nodules represent a volume fraction of 12% and have an average count of 75/mm^2.

2.2- Microscopy and X-Ray Analysis

Specimens were polished by using standard metallographic techniques and etched with the 2% nital solution. Light optical microscope (Nikon, FX-35DX) was used for microstrucural

analysis. The phases and constituents of the matrix were identified by using Cu-Kα radiation with Ni filter at 40,000 volt difference between a tungsten filament and copper target 30mA. X-Ray diffraction (XRD) analysis was performed to estimate the austenite content, the percentage of carbon in austenite, and their product $X_\gamma C_\gamma$ following the procedure of Rundman and Klug. And so the particle size d_α, have been investigated by using the Scherrer formula. The XRD equipment used in this work is Philips–binary (scan) of a PW.1800. A diffraction pattern records the X-ray intensity as a function of 2-theta angle. All the diffraction patterns were prepared as step-scans. To run a step-scan set the tube voltage and current, and enter the following parameters should be entered:

Start Position [2°Th.]	2.0100
End Position [2°Th.]	99.9900
Step Size [2°Th.]	0.0200
Scan Step Time [s]	0.5000

Once started, the goniometer moves through its range, stopping at each step for the allotted time. The X-ray counts at each step are saved to a file on the computer. The profiles were analyzed on a computer to obtain the peak positions and the integrated intensity of (111), (220) and (311) peaks of austenite and (110) and (211) peaks of ferrite. The volume fraction of ferrite X_α and austenite X_γ were determined by using the direct comparison method for a mixture of ferrite and austenite, the direct comparison expression can be written as[7]:

$$\frac{I_\gamma}{I_\alpha} = \frac{R_\gamma X_\gamma}{R_\alpha X_\alpha} \qquad (1)$$

Where I_γ is the integrated intensity from a given reflection plane of austenite phase γ; I_α is the integrated intensity from a given plane of ferrite α phase and R_γ and R_α are constants obtained from following R value expression [7]:

$$R=1/v^2 (|F|^2 pL) e^{-2M} \qquad (2)$$

Where v is the volume of unit cell; *F* is the structure factor; *p* is the multiplicity factor; *L* is the Lorentz-polarization factor; and (e^{-2M}) is the temperature factor. The quantity M depends on the amplitude of thermal vibration and scattering angle. The carbon content of retained austenite calculated according to angular positions of the FCC austenite peaks, C_γ can be calculated from equation (3):

$$C_\gamma = (a_\gamma - 3.555) / 0.044 \qquad (3)$$

Hence $a_\gamma = 0.3555 + 0.0044\ C_\gamma$, where a_γ is the lattice parameter of austenite in last equation in nano meter [8]. An estimate of ferritic cell size (d_α) obtained from the x-ray diffraction profile from the breadth of the {211} diffractometer peaks of ferrite using the Scherrer formula [9].

$$d_\alpha = \frac{0.9\lambda}{\beta \cos\theta} \qquad (4)$$

Where λ is the wave length, β is the breadth of the (211) peak of ferrite at half height in radians and θ is the Bragg angle.

3- Discussion of Results **a-** The effect of austenitization temperature on the microstructure has been studied by comparing the micrographs in figures (1) and (2) for similar

austenitization times of 15, 30, 60, 120, and 180 min. The results indicate that the increase in the austenitization temperature from 900-1000°C influences the austempered microstructure in various ways, the austempered microstructure has coarsened, the volume fraction of retained austenite has increased, and the amount of blocky retained austenite has detected.

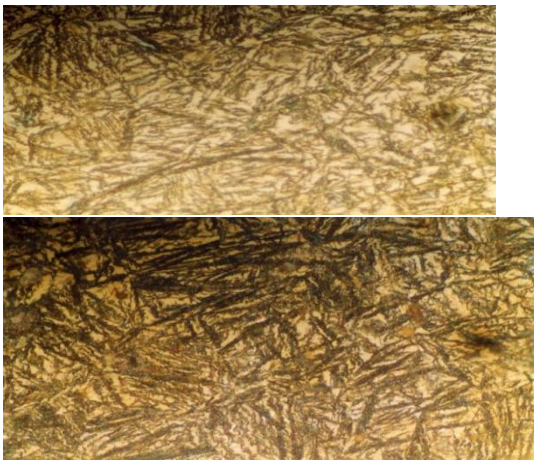

(a) (b)

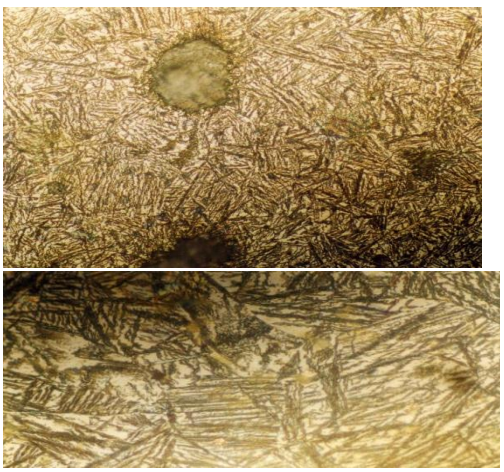

(c) (d)

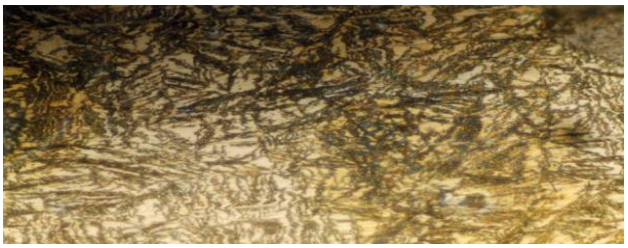

(e)

Figure (1) Microstructures of an alloyed ADI samples at T_γ=900°C, for different t_γ: (a) 15, (b) 30, (c) 60, (d) 120, and (e) 180min, 15

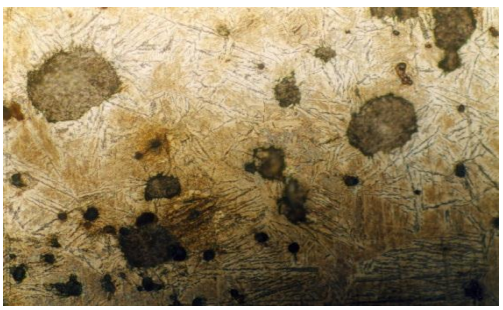

00x.

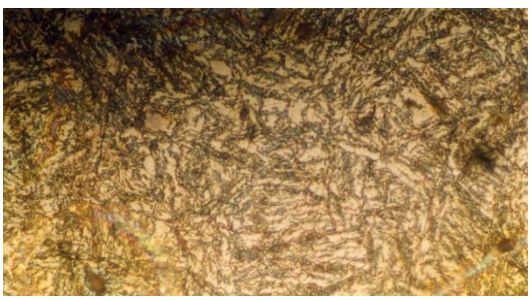

(a) (b)

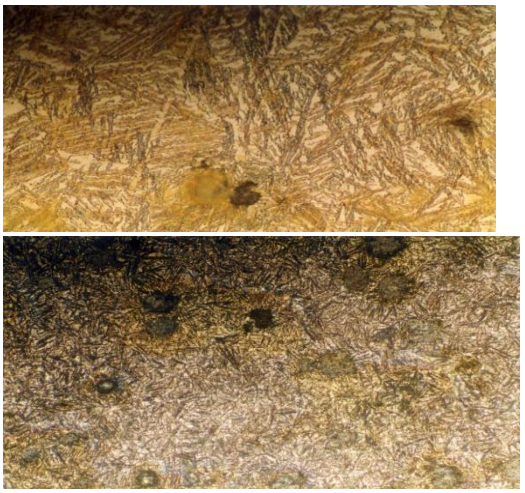

(c) (d)

(e)

Figure (2) Microstructures of an alloyed ADI samples at T_γ=1000°C, for different t_γ: (a) 15, (b) 30, (c) 60, (d) 120, and (e) 180min, 600x.

b- The austempered microstructure of ADI formed by austenitizing at 1000°C for 15min consists of acicular ferrite in the form of fine needles distributed more uniformly throughout the structure, with the retained austenite appearing as silvers in between these ferrite needles. At higher austenitizing temperature and lower time, the nucleation of ferrite may be expected to be faster, but the carbon rejected during formation of ausferrite may diffuse only to shorter

distances thereby forming fine ferrite and austenite. During austenitization, the cast microstructure transforms to austenite, and its carbon content depends upon the initial microstructure including nodule size and nodule count, austenitization temperature, and time. In a fully ferritic matrix, carbon diffuses only from the graphite nodules to the surrounding matrix during austenitization. The graphite nodules are the only source of carbon, and consequently, the carbon diffusion distances involved during solution treatment may be relatively large. This is nearly true because very little carbon can be attained from the small quantities of spheroidized carbides present. Consequently, full austenitization requires either very long solution treatment cycles or a very high carbon diffusion rate. However, in a pearlitic matrix, the graphite nodule and cementite of pearlite contribute to the carbon enrichment of the mother austenite, which is subsequently subjected to austempering at a given temperature, taking place in two stages. Figure (1) shows the variation of austempered microstructure with austenitization at 900°C for time periods 15, 30, 60, 120 and 180 min. The austempered microstructures consist of acicular ferrite and retained austenite but it is non-uniform when austempered after 15, 30 min of austenitization at 900°C. As the time of austenitization is increased to 60, 120, and 180 min, the acicular ferrite and retained austenite get distributed more uniformly due to homogeneous carbon content of austenite in the matrix. However, for the same austempering treatment after austnitization at 1000°C for different times, the microstructures are significantly different from those austenitization at 900°C, figure (2). The austempered structure is uniform for 180 min of austenitization, as the carbon content has become uniform after 180 min due to higher diffusion coefficient at 900, 1000°C, as the time of austenitization is increased, the

resulting austempered microstructure becomes coarser, which may be attributed to grain growth of austenite resulting in lower rate of heterogeneous nucleation of ferrite. Thus, a coarse structure results with retained austenite present as large blocky areas. The number of ferrite platelets is much greater for the samples austenitized at 900°C then those at 1000°C for the same austempering condition, of 360°C for 180 min as observed in figure (1), and (2). As described former, the XRD measurements allowed estimates to be made of the austenite lattice parameter, and then the austenite carbon content of each sample of ADI, figure (3) shows how the carbon content of the retained austenite varied with austenitizing conditions.

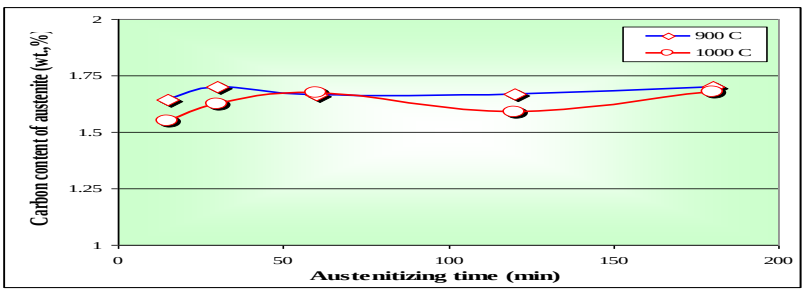

Figure (3) Effect of austenitizing conditions on carbon content of austenite in ADI samples

This agreed with figure (4) which show the schematic free energy- composition diagram [10], thus at lower austenitizing temperature (900°C), a greater driving force can affect the rate of stage I in two ways: the number of ferrite nuclei may increase directly and / or the activity gradient driving carbon diffusion may increase, this is happened. Lowers the driving force controlling the transformation of austenite to ausferrite from ab to a'b', the driving force reduction is responsible for the decrease in the number of ferrite nuclei formed and the slower growth along the ferrite platelet. Therefore, as shown in figure (2) increasing the austenitizing temperature to

1000°C leads to structures containing a high percentage of large austenite grains.

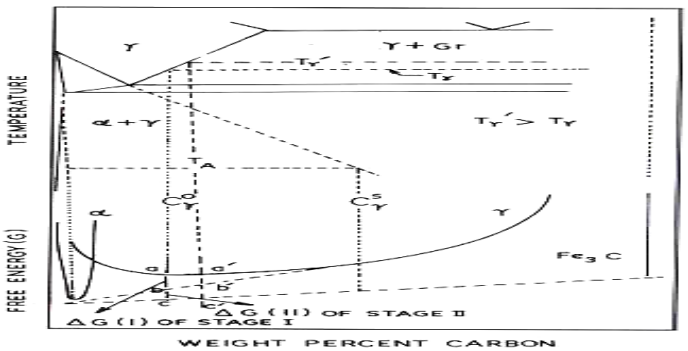

Figure (4) Schematic free energy- composition diagram indicating the driving force for stage [I] and stage [II] of austempering [10].

c- Another results obtained by calculating volume fraction of austenite by using direct comparison method show that: increasing both times and temperatures of austenitizing followed by increasing in austenite content figure (5) shows a plot of the volume fraction of austenite against the austenitizing conditions. The austenite content was observed to increase with increasing austenitizing temperatures.

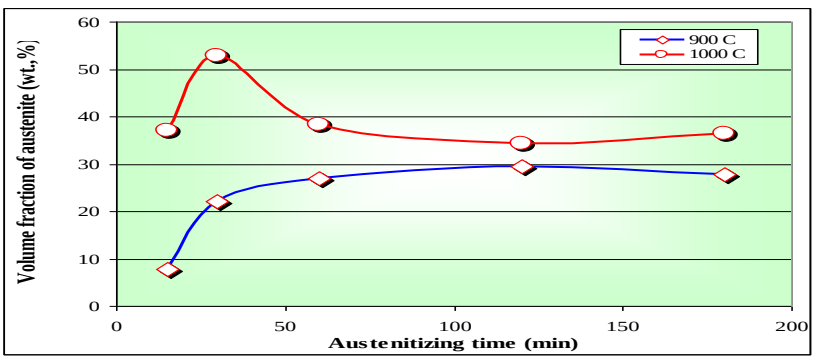

Figure (5) Effect of austenitizing conditions on volume fraction of austenite calculated by direct comparison method.

d- A Computer program employed at the Libyan petroleum Institute is used to carry out the measurements for quantitative analysis automatically for each sample, as is shown in figure (6).

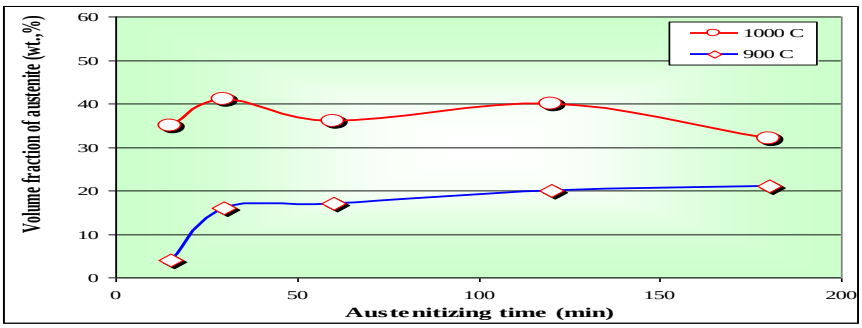

Figure (6) Effect of austenitizing conditions on volume fraction measured by diffractometer.

e- From traditional data, the yield strength of ADI depends on the fineness of ferrite and austenite, therefore the fracture toughness, fatigue strength of ADI have been observed to depend on the parameter (austenitic carbon content, $X_\gamma C_\gamma$). As shown in figure (7) where the austenitic carbon content ($X_\gamma C_\gamma$), i.e. the total carbon in austenite is plotted against the austenitizing time.

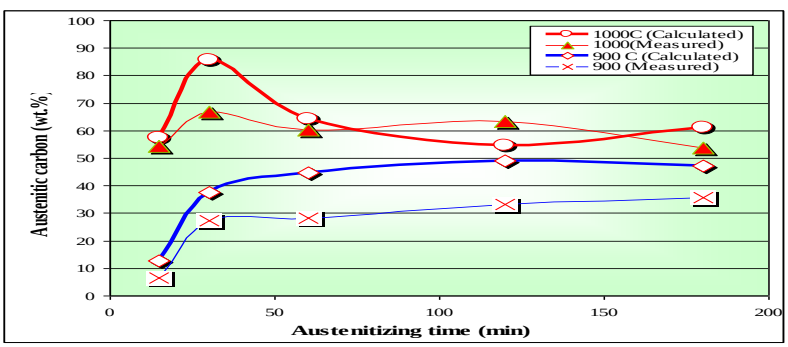

Figure (7) Effect of austenitizing conditions on austenitic carbon (calculated & measured).

f- Figure (8)shows the variation of the ferritic cell size (d_α) with the austenitizing time at 900ºC.

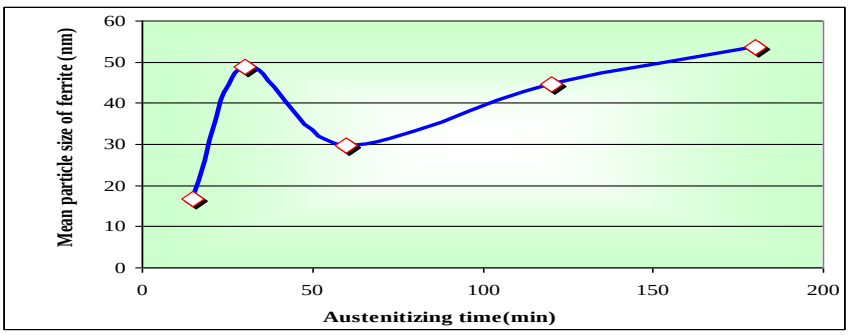

Figure (8) Influence of austenitizing time on ferritic cell size at 900ºC.

4- Conclusions

The following conclusions can be drawn:

- The amount of the carbon content in austenite increases with increasing austenitizing time, and retained austenite increases with increasing both the time and temperatures of austenitization.
- The volume fraction of retained austenite X_γ, its carbon content C_γ, and $X_\gamma C_\gamma$ are small at short austenitizing time.
- In a ferritic matrix structure, significantly more time is required to reach equilibrium carbon content in the mother austenite. This is attributed to the larger carbon diffusion distances and the presence of copper, which segregates to the graphite- metal interface and creates a carbon diffusion barrier.
- The austenitizing conditions not only affect the morphology of ferrite but also that of retained austenite. Austenite appears to exist in the form of films between ferrite needles, as well as in blocky morphology.
- In ADI austenitizing at higher temperatures, it has coarser or feathery ferrite and austenite and by last

knowledge, this reduces the yield and tensile strengths but imparts higher ductility.

- Increasing T_γ from 900 to 1000°C decreases the free energy controlling the transformation of austenite to ferrite and high carbon austenite. Less ferrite nuclei are formed at 1000°C, and the resulting structure is coarser and contains more blocky type austenite.
- The austenitizing time corresponding to most desirable austempered microstructure is 180 followed by 120 min.
- The austenitizing treatments exert well-pronounced effects upon the microstructure, then mechanical properties of austempered ductile iron.
- Previous results [11] indicated that the austenitizing temperature T_γ, and time t_γ, have a significant effect on the mechanical properties for the same alloys, this can be attributed to the influence of these variables on the carbon kinetics.

REFERENCES

[1] B. Imasogie, A. Afonja. J. Ali, "Properties of ductile cast iron modularized with multiple calcium- magnesium-based alloy," Mat. Sci. Tech., 16, 194-201 (2000).

[2] C. Hsu, S. Lee, H. Feng, and Y. Shey, "The effect of testing temperature on the fracture toughness of austempered ductile cast iron," Met. Trans., A32. 295-303 (2001).

[3] p. Rao and S. Putatunda, "Influence of microstructure on fracture toughness of austempered ductile cast iron," Met. Trans., A28, 1457-1470 (1997).

[4] J. Aranzabai, I. Gutierrez, and J.J. Urcola, "Influence of heat treatment on microstructure of austempered ductile cast iron," Mat. Sci, Tech., 10, 728-737 (1994).

[5] J. Achary and D. Venugopalan, " Microstructural development and austempering kinetics of ductile iron during thermomechanical processing." Met. Trans., A13, 2575-2583 (2000).

[6] S. K. Putatunda: Mater.Sci.Eng. A315 (2001), PP.70 -80. Summary Plus / Article / Journal Format-PDF (832K).

[7] J. Yang, S.K. Putatunda: "Improvement in strength and toughness of austempered ductile cast iron by two-step austempering process", J.Mater. Design, 2004, 25(3), pp.219-230.

[8] Z. M. EI-Baradie, M. M. Ibrahim, I. A. EISisy, A. A. Abd EI-Hakeem: "Austempering of Spheroidal Graphite Cast Iron,"J.Mats.Sci.,40(4),2004,p.523-528.

[9] B.D. Cullity, "Elements of X-ray diffraction".2nd Edition. London, Addison-Wesley, 1978.

[10] Uma Batra, S. Ray, and S. R. Prabhakar, "Effect of Austenitization on Austempering of copper Alloyed Ductile Iron," J. Mater. Eng. Performance, 2003, 12(5),pp.597-601.

[11] M. Alaalam: "Effect of initial matrix structure and Austenitizing Conditions on microstructure and mechanical Properties of Cu, Ni Austempered Ductile Iron " ,Ph. Thesis,1997, university of Malta.

Influence of Design Tip Speed Ratio and Rated Wind Speed on Energy Yield of Horizontal Wind Turbine

Mohamed Ali Naili

Abstract Wind turbines are the means of converting wind energy into electrical energy. It is not unexpected that certain brands of horizontal wind turbines are optimally designed for certain wind speed regimes prevailing at certain sites. It has been the objective of this study to find out whether it is possible to design a wind turbine that is more suitable for a site of lower annual mean wind speed such as the western coast of Libya. In achieving this objective, use was made of a typical wind turbine aerodynamic design and performance analysis procedure together with actual wind speed data recorded at the city of Misurata.

Based on the annual wind energy yield obtained from different designs of wind turbines having different rated wind speeds and different blade design tip speed ratios, this study indicates that the decrease of the rated wind speed leads to a continuous increase of annual energy yield as well as an increase of the cost of the wind turbine. Therefore the optimum value of rated wind speed for this site may only be determined as a compromise between added wind energy yield and added cost. Moreover, for any given rated wind speed this study indicates that a blade design tip speed ratio equal to six seems to be the optimum value for the given site.

Objective It is not unexpected that certain brands of horizontal wind turbines are optimally designed for a certain wind speed regime or regimes prevailing at a certain areas of the world. In other words, the wind turbine is designed such that it would work most efficiently if it were installed at a site of a given wind speed regime. On the other hand it would work less efficiently if it were installed at a site of a different wind speed regime. It is

thus expected that several wind turbines that are made in Europe were designed to suit the wind speed regimes prevailing in that area. Since the annual mean wind speed in Europe is relatively higher than the corresponding value in Libya, it is not unexpected that European-made wind turbines would work less efficiently here.

The objective of this study is to find out whether it is possible to design a wind turbine that is most suitable for a wind regime of lower annual mean wind speed. In achieving this objective, usage was made of a typical wind turbine aerodynamic design procedure together with actual wind speed data of a certain Libyan site. Analysis and comparison of the final results were based on the annual wind energy yield at the site obtained from the different wind turbines.

The P(V) curve The power output of the wind turbine varies with the wind speed as shown schematically in Figure (1). It is noted from this figure that the wind turbine does not produce any power until the wind speed , V, exceeds what is termed the 'cut-in wind speed', V_C. Beyond this velocity the power output, P, increases as V increases. When the wind speed reaches a value termed the 'rated wind speed', V_r, the wind turbine produces its rated power output, P_r. From thereon, as the wind speed increases the power output remains constant. Once V reaches a value termed the 'furling wind speed', V_f, the value of P becomes zero [6].

It is expected that wind turbines commercially available in Europe, for example, are more suitable for such a continent where wind speed patterns show relatively higher annual average wind speeds. It is well known that the annual average wind speed in Libya is relatively low, so it is not unexpected that the performance of those turbines in Libya will be less efficient than if operated in Europe. The P(V) curve is constructed from the $C_P(\lambda_0)$ curve of the wind rotor plus the $P(\omega)$ of the electrical

generator to be employed, where 'ω' represents the rotational speed of the generator. The wind turbine power curve strongly depends on the wind rotor $C_P(\lambda_0)$ curve.

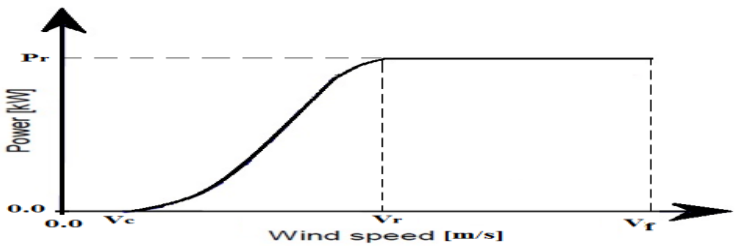

Fig. (1): Schematic drawing of typical P(V) curve [8].

Analytic procedure In order to determine the annual energy yield at the selected site for any of the case studies, a sequence of computational procedures were followed. This sequence consisted of wind rotor aerodynamic design followed by performance analysis of the designed rotor and then the construction of the power curve for the resulting wind turbine.

Wind energy yield at a site

1. Wind speed data For the sake of this study, raw wind speed data recorded by Libyan National Meteorological center at the city of Misurata were employed. This data set contains measurements of mean wind speed at 3-hours intervals taken at a height of 10 meters above ground level. The data was recorded in 2010 and covers a period of 12 months. It is found that mean wind speed for this site was 5.3 m/s.

2. Method of evaluation

By definition, the power P is given by:

$$P = \frac{dE}{dt} \quad \text{(Joule / sec)} \quad \text{or (Watt)} \qquad \ldots\ldots\ldots\ldots\ldots (1)$$

Hence, $E = \int P(t)dt$ …… (2)

Now given the power curve of the wind turbine P(v), and given the raw wind data V(t), the integral in (2) above may thus be evaluated as follows

$$E \approx \sum_{i=1}^{i=N} Pi(Vi)\,\Delta t \quad \text{…… (3)}$$

Where:

N = total number of wind speed data points.

Δt = 3 hours in this case.

$P_i(V_i)$ = electrical power output when $V=V_i$

The units of E would be (KW-hr), since P is evaluated in units of (KW).

Since N is large, the summation in (3) would be a good approximation to the integral given by (2). Moreover, since the proper evaluation of energy yield at the selected site is not the objective of this study, this approximation is thus justified.

Description of cases Table (1) below shows a total of thirty cases studied with a symbol assigned to each one. The letter 'T' stands for the design tip speed ratio while 'V' stands for the rated wind speed. So for example the symbol 'T5V11' refers to the case in which λ_{0D} and V_r were equal 5 and 11 respectively. Normally, values of λ_{0D} of around 7 are used in commercially available wind turbines. However, for the purposes of this study lower values of λ_{0D} were investigated, namely 6, 5 and 4 as shown in table (1). Moreover, it is noticed that values of rated wind speed of a substantial number of existing horizontal axis wind turbines lie in a range of 12 to 14 (m/s). Once again, lower values of V_r, namely 11 and 10 were investigated in order to study their effect on energy yield at sites of generally lower annual mean wind speeds.

Table (1): Cases studied with their respective symbols

V_r (m/s)	λ_{0D}				
	4	5	6	7	8
10	T4V10	T5V10	T6V10	T7V10	T8V10
11	T4V11	T5V11	T6V11	T7V11	T8V11
12	T4V12	T5V12	T6V12	T7V12	T8V12
13	T4V13	T5V13	T6V13	T7V13	T8V13
14	T4V14	T5V14	T6V14	T7V14	T8V14
15	T4V15	T5V15	T6V15	T7V15	T8V15

Wind rotor design For the given values of ρ, η_{GB}, η_{EG}, P_r, Cp_r , the radius of the rotor, R, may be determined for any given value of the rated wind speed, V_r , using the mathematical relationship.

$$P_r = \frac{1}{2}\rho\, Cp_r \pi\, R^2\, V_r^3 \eta_{GB}\, \eta_{EG}$$

Since the rotor diameter varies inversely with the square of rated wind speed, the blade chord distribution for any given design tip speed ratio is determined in non-dimensional form, namely as C(r/R). In this manner, for a given value of design tip speed ratio one obtains a group of "geometrically similar blades" though with different actual values of rotor radii and actual values of chord distributions. Consequently, the $Cp(\lambda_0)$ curves for the whole group (with the same λ_{0D}) are absolutely identical.

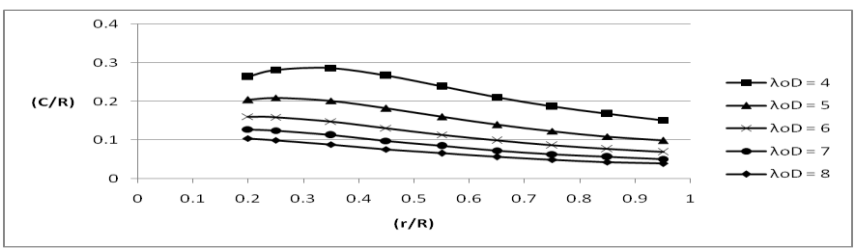

~~Fig. (2): Influence of λ_{0D} on blade chord distribution.~~

Wind rotor performance. Cp(λ_0) curves for the five wind rotor geometries were obtained as shown in Fig.(4). In performing the above procedure, use was made of the aerodynamic data contained which presents variation of lift and drag force coefficients as functions of angle of attack for the airfoil used, namely NACA 0012.

As can be seen from Fig.(4) the $C_p(\lambda_0)$ curves follow the normal trend. The power coefficient increases with the increase of tip speed ratio and reaches a maximum value ranging from 0.46 to 0.475 and then falls down continuously. It can be seenthat the value of λ_0 at which Cp attains its maximum value increases as λ_{0D} increases. This is mainly due to the fact that the rotor design is based on maximizing the local value of Cp at the selected design tip speed ratio. It is also noticed that the operational range increases slightly with the increase of λ_{0D}.

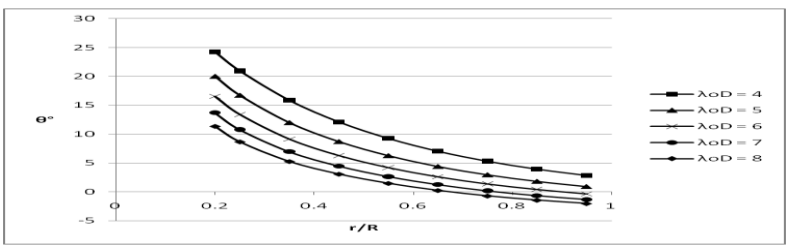

Fig.(3): Influence of λ_{0D} on twist angle distribution.

Wind turbine power curve The wind turbine power curve was constructed via the matching of the wind rotor power characteristics with nominal electrical generator power characteristics.

For each one of the five distinct rotor geometries, six different rotor diameters were employed corresponding to the six different rated wind speeds selected, namely 10, 11, 12, 13, 14 and 15 (m/s). In this manner six different wind turbine power curves were obtained for each of the five values of λ_{0D}. It is noted that in order to obtain any one of these power curves, the same nominal electrical generator

power characteristics were employed. The same results are presented in the form of power curves for a given value of V_r and different values of λ_{0D}.

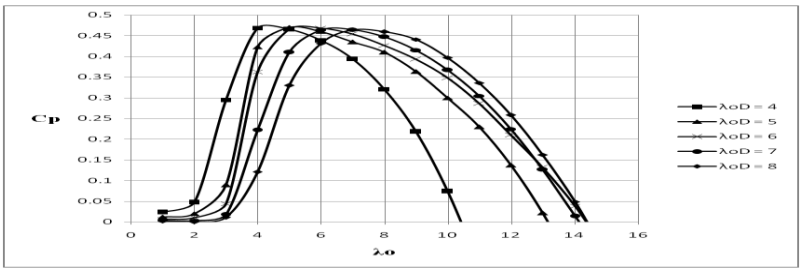

Fig. (4):Variation of power coefficient with changes in tip speed ratio.

Wind energy yield. In order to investigate the effect of rated wind speed as well as the effect of rotor design tip speed ratio on energy yield, raw wind speed data collected at the city of Misurata were employed.

1. Effect of rated wind speed

Fig. (5) presents curves of annual wind energy yield, E_{an}, as a f unction of rated wind speed for given values of λ_{0D}. It can be seen from this figure that the increase of V_r leads to a continuous decrease of E_{an} for all cases of λ_{0D}. This result is due to the shift of the power curve to the right as Vr increases. However, it must be noted that though decreasing the rated wind speed leads to increased wind energy yield, the substantial increase in the rotor diameter would certainly lead to increased cost of the rotor itself plus the cost of other wind turbine parts such as the tower and the mechanical parts of the control system. Therefore, to determine the optimum rated wind speed for a site, one has to analyze the added costs resulting from the reduction of Vr and weigh them against the gains in wind energy yield over the assumed life time of the wind turbine.

2. Effect of design tip speed ratio

Fig.(6) presents curves of E_{an}, as a function of λ_{0D} for given values of V_r. It can be seen from this figure that for any given value of rated wind speed, the annual energy yield increases with the increase of λ_{0D} up to a value of around 6. From thereon, the value of E_{an} decreases continuously. This is mainly due to manner in which the power curve changes with λ_{0D} for any fixed value of Vr. Thus for the given site, there seems to be an optimum design tip speed ratio of around 6 irrespective of the value of the rated wind speed.

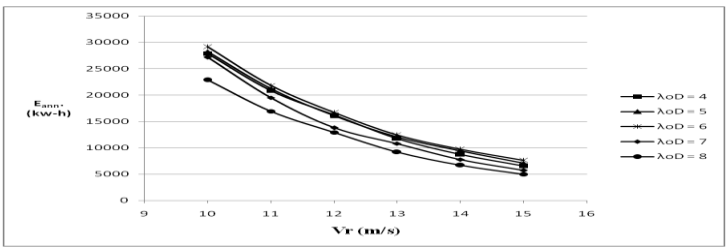

Fig. (5): Influence of λ_{0D} on annual energy yield for different values of V_r.

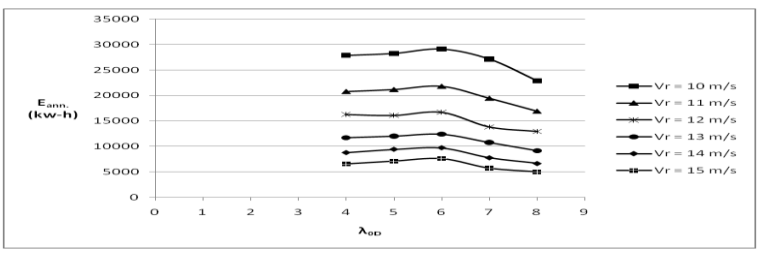

Fig. (6): Influence of V_r on annual energy yield for different values of λ_{0D}.

Conclusions From the foregoing discussion, the results of this study show that within the ranges of rated wind speed and blade design tip speed ratio explored and based on the analytical method employed the following conclusions may be drawn:

- F

  or the site employed in this study, the annual energy yield reaches a maximum at a value of design tip speed

ratio of around 6 irrespective of the value of the rated wind speed. This indicates that the optimum value of λ_{0D} for this site could well be equal to 6.

- The decrease of rated wind speed leads to a continuous increase of annual energy yield as well as rotor radius for any given blade design tip speed ratio. This implies that no optimum value of V_r may thus easily be identified.

- Since decreasing V_r would lead to an increase in rotor radius which in turn would lead to an increase in the cost of the wind turbine, therefore the optimum value of V_r for a given site may only be determined as a compromise between added annual energy yield and added wind turbine cost.

From the foregoing statements it is clear that in order to determine whether it is possible to design a wind turbine that is most suitable for a wind regime of lower annual mean wind speed one has to supplement the results of the current study with corresponding results of another study that primarily deals with cost analysis resulting from changes of rotor diameter. Such a study is well beyond the scope of this thesis.

References

1. Gary L. Johnson, “Wind energy systems”, Pub. Manhattan KS, 2001.

2. Sathyajith Mathew, “Wind energy, fundamentals, resource analysis and economics”, Pub. Krips bv, 2006.

3. Mukund R. Patel, “Wind & solar power systems”, CRC Press LLC, 1999.

4. J. F. Manwell, J. G. McGowan, and A. L. Rogers, "Wind energy explained", John Wiley & Sons Ltd., 2002.

5. IEC 61400-1, "Wind turbines- part 1: Design requirements", International Electrotechnical Commission, 2005.

6. NV/ Risφ, "Guide lines for design of wind turbines", Jydsk Centraltrykkeri, 2002.

7. mmanuel Y. Osei, "Technical & financial assessment of a 50 MW wind power plant in Ghana", Msc thesis, Kwame Nkrumah University, Ghana, 2010.

8. desire Le Gourieres, "Wind power plants theory and design", Pergamon Press Ltd., 1982.

9. rant Ingram, "Wind turbine blade analysis using the BEM method", technical report, Durham University, 2011.

10. M. Ragheb, "Optimal rotor tip speed ratio", technical report, Springer Verlag, Germany, 2011.

11. George Sterzinger, and Matt Svrcek, "Wind turbine development: location of manufacturing activity", department of energy, USA, 2004.

12. Tony Burton, David Sharpe, Nick Jenkins, and Ervin Bossanyi, "Wind energy handbook", John Wiley & Sons Ltd., 2001.

13. National Renewable Energy Action Plan,2009, Ireland.

14. Global wind report: annual market update 2013, GWEC.

15. Worldwide electricity production from renewable energy sources: stats and figures series, 2013, GWEC.

16. Robert E. S., and Paul C. Klimas, "Aerodynamic characteristics of seven symmetrical airfoils", spring field, 1981.

17. Libyan National Meteorological Center, (LNMC), Tripoli, Libya.

Slow release of entrapped *Azospirillum brasilense* cells

Fadel M.Belaid[1]., Nagah S.Abubaker[2]. and Hesham M. A. El-Komy

Omar Al-Mukhtar Faculty of science, Department of Botany University,

[2]Esra92nn@gmail.com[1]fadelblaeed@gmail.com

Abstract

In this study *Azospirillum brasilense* st.was formulated in alginate pellets to study the slow release and survival of bacteria from alginate beads. Recorded in this study high number of *A. brasilense* cells were released from alginate pellets when starch was used as adjuvant, and recorded $38.5x10^4$ and $10.7x10^4$ cfu/g bead at initial and 8th day of sampling, respectively and The least cell number of *Azospirillum* was released by immobilization in alginate alone without any addition, recording $27.5x10^4$-$13.1x10^3$ cfu/g bead at initial and 8th day of sampling, respectively.
Keywords: *Azospirillum brasilense* , survival, alginate pellets

1.INTER0DUCTION

The encapsulation of cells methods was the best methods and most safe introduce *Azospirillum* in the soil where they are protected from environmental conditions and organisms competitors and increase their persistence and survival in the soil. (Kumaresan and Reetha, 2012). *Azospirillum* bacteria as plant growth promoting bacteria PGPB, where it has a positive impact on plant growth through its impact on root through nitrogen fixation and production of phytohormones and their survival depends on the soil on abiotic and biotic factors (Van Veen *et al.,* 1997). the PGPB population in rhizosphere was inhibited by the decreased in the number of inoculated bacteria (Bashan, 1998). carrier bacteria on the gel material is one of the most successful methods for the introduction of bacteria in the soil (Vassilev *et al*., 2001). The primary goal of encapsulation PGPB the protection of vital and non-vital factors and RELEASE PGPB gradually to the soil to be able to colonize the roots (Bashan *et al.,* 2002; Vassilev *et al.,* 2001; El-Komy, 2001; 2005). and abiotic stresses such as the inhibitory effect of toxic compounds (Smit *et al.,* 1996; Cassidy *et al.,* 1997), to support the survival and activity Physiological (Weir *et al.,* 1995; Trevors *et al.,* 1993), In the present study, experiments were conducted to develop the

gel based formulation of *Azospirillum brasilense* bioinoculant by enriched with different additives *viz.*, skimmed milk powder and starch

2.MATERIALS AND METHODS

Microorganisms

A. brasilense isolate has been obtained from free soil in Hai Al-salam district of Derna, Libya

Immobilization of *Azospirillum brasilense* isolate in alginate pellets:

A. brasilense isolate was immobilized by entrapment in 2% Ca-alginate. Cells encapsulated in alginate pellets were prepared by using the method applied at our laboratory (Shaban and El-Komy, 2000; El-Komy, 2001; 2005). Briefly, 25 ml of bacteria cell suspension under aseptic condition were added to75 ml of sterile alginate solution to obtain a final concentration of 2% alginate. In some cases skim- milk (2.5%w.v) or starch (2.5%) was added as adjuvant. The mixture was vigorously stirred to allow a homogenous dissolution of alginate. Then the mixture was extruded through sterile plastic nozzle with a diameter of 1mm and the resulting drops were then projected into sterile 6 g/1 $CaCl_2$ solution forming small calcium alginate matrix beads (2mm, mean diameter) entrapping bacterial cells. The beads were maintained in $CaCl_2$ solution at room temperature for additional 1-2h to obtain regular solid beads. The $CaCl_2$ solution was pumped out, and the beads were washed twice with sterilized distilled water. Fresh beads were either used directly as fresh, or kept at 4-5°C in sealed flacks for several days. Bacterial cells within 0.1g pellets were calculated after dissolving the pellets in phosphate buffer (pH7) solution by diluted agar plate.

Slow release of entrapped *Azospirillum brasilense* cells

A portion of 30 washed beads containing immobilized bacteria was transferred into 75 ml of sterile saline solution (0.1 % W/V NaCl) and gently shaken at 30°C for 24 h. Then triplicate samples of 0.5 ml of saline solution were collected, and the number of released bacteria was determined by the plate count method on nutrient agar plates. Then the pellets were rinsed twice in sterile water and transferred into a fresh saline solution, and the procedure was repeated after an additional 24 h up to 8 days.

3.RESULTS AND DISCUSSION

Slow release of *A. brasilense* (F_3) cells from alginate beads enriched with various additives:

The release of *Azospirillum* cells from gel formulation was assessed up eight days . It was found that decrease of *Azospirillum* released from alginate beads from initial to 8^{ht} day of screening. Among the various treatments, higher amount of *Azospirillum* cells ($38.5x10^4$ and $10.7x10^4$ cfu/g bead) was released in Alginate + starch at initial and 8^{th} day of sampling, respectively, followed by Alginate formulation with

skim milk addition

($29.0x10^4 – 15.0x10^3$ cfu/g). The lower amount of *Azospirillum* cells ($27.5x10^4$ -$13.1x10^3$ cfu/g bead) alginate alone gel formulation of initial and 8^{th} day of sampling, respectively.

Entrapment of microbial cells has been reported to improve their metabolic activities and enhance the production of several hydrolyic enzymes (El-Katatny *et al.,* 2004; El-Komy, 2005). Alginate immobilization has also been used as inoculant for plant growth promoting bacteria for over more than two decades (Bashan, 1986). The gel-like matrix allows the cells to remain viable and with its catalytic ability for longer duration (Bashan and Levanony, 1988 ;El-Komy, 2001). Moreover in the present study. The release of *A. brasilense* from alginate formulations with different additives (starch or skim milk) supported higher *Azospirillum* number released from the preparations when compared alginate formulations alone without any adjuvants. Sodium alginate with starch or skim milk might provide nutrients facilitating the bacterial multiplication within the bead. These findings are in accordance with many researches shown that the addition of adjuvants such as humic acid, starch, cellulose or skim milk is presumed to enhance the stability and provide protection and nutrition to the encapsulated microorganisms (Bashan, 1986 , Shaban and El-Komy, 2000 ; El-Katatny *et al*., 2004 , Kumaresan and Reetha, 2012).

Table .1: Slow release of alginate immobilized *Azospirillum* strain.

Alginate beads with adjuvant	Initial	2days	4days	6days	8days
Alginate	$27.5 X 10^4$ (5.44)	$18.0 X10^3$ (4.25)	$16.4 X10^3$ (4.20)	$16.1 X10^3$ (4.20)	$13.1X10^3$ (4.11)
Alginate +S.milk	$29.0 X10^4$ (5.46)	$18.5 X10^3$ (4.27)	$18.5 X10^3$ (4.26)	$18.0X10^3$ (4.25)	$15.0 X10^3$ (4.18)
Alginate + Starch	$38.5 X10^4$ (5.58)	$12.5 X10^4$ (5.10)	$12.0 X10^4$ (5.07)	$11.2 X10^4$ (5.04)	$10.7 X10^4$ (5.02)

Azospirillum population (CFU /g bead), and values in parenthesis are log No.

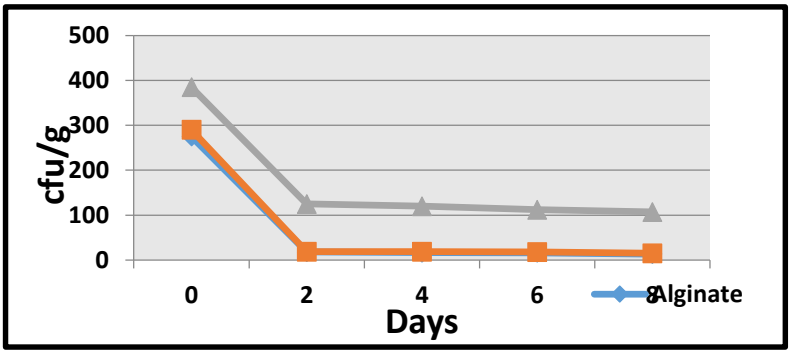

Fig.1: Slow release of alginate immobilized *Azospirillum* strain **.**

REFRENCES

Bashan Y, Hernandez JP, Levya LA, Bacilio M. (2002). Alginate microbeads as inoculant carriers for plant growth-promoting bacteria. Biol Fertil Soils 35:359–368.
Bashan, Y. (1998). Inoculants of plant growth-promoting bacteria for use in agriculture. FEMS Microbiology rev. 3(2): 729-770.
Bashan, Y.; Levanony, H. (1988): Adsorption of the rhizosphere bacterium *Azospirillum brasilense* Cd to soil, sand and peat particles. J. Gen. Microbiol 134:1811-1820.

Cassidy MB, Lee H, Trevors JT. (1997). Survival and activity of lac-lux marked Pseudomonas aeruginosa UG2Lr cells in encapsulated kcarageenan over 4 years at 48C. J Microbiol Meth 30:167–170.
El-Katatny, M.S.; El-Komy, H.M.; Shaban, G.M.; Hetta, A.M.; El-Katatny, M.H. (2004): Effect of benomyl on chitinase and 0-1,3--glucanase production by free and alginate encapsulated *Trichoderma harzianum.* Food Technol. Biotechnol. *42*: 83-88.

El-Komy, H. (2001): Survival of and wheat – root colonization by alginate encapsulated *Herbaspirillum* spp. Folia. Microbiol. 46: 25-30.

El-Komy, H. (2005): Coimmobilization of *Azospirillum lipoferum* and *Bacillus megaterium* for successful phosphorus and nitrogen nutrition of wheat plants. Food Technol. Biotechnol. 43: 19-27.

Kumaresan, G. and Reetha, D. (2012): Development of gel based formulation enriched with different additives of *Azospirillum* inoculants. Int. J. Recent Sci. Res. 3: 923-927.

Shaban, G. and El-Komy, H. (2000): Survival and proliferation of alginate encapsulated *Trichoderma* in Egyptian soil. Mycopath. 151: 139-146.

Smit E, Wolters AC, Lee H, Trevors JT, van Elsas JD. (1996). Interaction between a genetically marked Pseudomonas fluorescens strain and bacteriophage øR2f in soil: Effects of nutrients, alginate encapsulation, and the wheat rhizosphere. Microb Ecol 31:125–140.

Trevors JT, van Elsas JD, Lee H, Wolters AC. (1993). Survival of alginate encapsulated Pseudomonas fluorescens cells in soil. Appl Microbiol Biotechnol 39:637–643.

Van Veen, J.A., Overbeek, L.S., Van Elsas, J.D., (1997). Fate and activity of microorganisms introduced into soil. Microbiol. Mol.Biol. Rev. 61: 121–135.

Vassilev N, Vassileva M, Azcon R, Medina A. (2001). Application of free and Ca-alginate entrapped Glomus deserticola and Yarowia lipolytica in soil-plant system. J Biotechnol 91:237–242.

Weir SC, Dupuis SP, Providenti MA, Lee H, Trevors JT. (1995). Nutrient enhanced survival of and phenanthrene mineralization by alginate encapsulated and free Pseudomonas sp. UG14Lr cells in creosotecontaminated soil slurries. Appl Microbiol Biotechnol 43:946–951.